Title
Burn depth determination by high-speed fiber-based polarization-sensitive optical coherence tomography at 1.3 μm

Authors
Park, Boris H
de Boer, Johannes F
Saxer, Christopher E
et al.

Publication Date
2000-04-28

DOI
10.1117/12.384163

Burn Depth Determination by High-Speed Fiber-Based Polarization Sensitive Optical Coherence Tomography at 1.3 micrometers

B. Hyle Park, Johannes F. de Boer, Chris Saxer, Shyam M. Srinivas, Huai-En L. Huang, Binh Q. Ngo, Zhongping Chen, J. Stuart Nelson.

Beckman Laser Institute and Medical Clinic,
Univ. of California, Irvine, 1002 Health Sciences Road East, Irvine, CA 92612.

ABSTRACT

Burn depth determination is a critical factor in the treatment of thermal injury. We have developed a technique, polarization sensitive optical coherence tomography (PS-OCT), to assess burn depth non-invasively. Thermal injury denatures collagen in human skin. PS-OCT is able to measure the resulting reduction in collagen birefringence using depth resolved changes in the polarization of light propagated and reflected from the sample. In a previous study, we used a free space PS-OCT system at 850 nm to image *in vivo* the skin of rats burned for various amounts of time. Using a high-speed system at 1.3 micrometers has the advantages of greater depth penetration and reduction of motion artifacts due to breathing and small movements of the animal. Stokes vectors were calculated for each point in the scans and the relative birefringence was determined using different incident polarization states. Birefringence was correlated with actual burn depth determined by histological analysis. Our results show a marked difference between normal tissue and even the slightest burn, and a consistent trend for various degrees of burns.

Keywords: birefringence, burn diagnosis, noninvasive imaging, optical biopsy, partial thickness burn, thermal injury

1. INTRODUCTION

Burns happen with startling frequency, with 5500 deaths (1991), 51,000 acute hospital admissions (average from 1991 to 1993), and 1.25 million total burn injuries (1992)[1], and range from minor household burns to life-threatening injuries of fire victims. Traditionally, burns are differentiated into first, second, and third degree. A first-degree burn shows damage in only the epidermal layer and is not considered a clinical problem. Second-degree burns show damage in to the upper dermis as well as the epidermis, and can heal by re-epithelialization. However, a third-degree burn is characterized by damage to the dermis that renders it unable to regenerate epithelium, necessitating more drastic procedures such as skin grafting. The difference between a second- and third-degree burn is not immediately identifiable to the naked eye. A physician will often have to wait 2-3 weeks before being able to make this distinction. Treatment plans can vary greatly depending on burn severity and become more effective the sooner they are instituted, making the ability to immediately determine the depth of burn injury critical.

A number of non-invasive methods have been developed to assess the depth of burn injury, including the use of indocyanine green dye fluorescence[2], vital dyes, fluorescein fluorometry, laser Doppler flowmetry (LDF), thermography, ultrasound, nuclear magnetic resonance imaging, and spectral analysis of light reflectance[3]. A great deal of research in this general area has been focused on LDF. Burned skin sustains damage to dermal arterioles, capillaries, and venules, resulting in reduced blood flow which can be detected by LDF[4]. However, due to the long coherence length laser sources required, LDF cannot provide a depth resolved image of blood flow, instead measuring perfusion over an entire volume of tissue. Problems with methodology and accuracy has limited the clinical use of LDF[5], as well as many of the other techniques mentioned, leaving observation as the standard for diagnosis[3].

Polarization sensitive optical coherence tomography (PS-OCT) is a recently developed imaging technique that uses coherence gating to image tissue birefringence with high spatial resolution[6, 7]. Birefringent materials alter the polarization state of light passing through them. Skin contains collagen, a weakly birefringent material. At temperatures between 56-65°C, collagen denatures and loses its birefringence[8]. By analyzing the polarization state of light reflected from various depths in a sample, PS-OCT is able to provide information on the amount and condition of collagen and, therefore, the depth of thermal injury. In a previous study[9], we were able to establish a correlation between PS-OCT measurements and depth of

In *Coherence Domain Optical Methods in Biomedical Science and Clinical Applications IV*,
Valery V. Tuchin, Joseph A. Izatt, James G. Fujimoto, Editors, Proceedings of SPIE
Vol. 3915 (2000) • 1605-7422/00/$15.00

thermal injury. This was done using a free space system with light at 850 nm. Scans 2 mm in depth and 6 mm laterally, were taken *in vivo* of both normal and burned portions of rat skin and required approximately twenty minutes to acquire. These measurements were subject to motion artifacts due to the breathing of the animal over the course of the measurement and limited penetration depth at 850 nm. We have developed a new high-speed fiber based system at 1.3 μm to address the problems of our previous study and improve the accuracy of our correlation.

2. MATERIALS AND METHODS

2.1. Animal model

The animal model used was female Sprague-Dawley rats (~300 g) housed in a pathogen free animal facility and given a commercial base diet and water *ad libitum*. The Institutional Animal Care and Use Committee at the University of California, Irvine, approved the experimental protocol. The rats were anaesthetized with an intraperitoneal injection of ketamine (87 mg/kg) and xylazine (13 mg/kg). After the animal's backs were shaved and treated with Nair lotion hair remover (Carter-Wallace, New York, NY), experimental burns were placed on the rat skin along the lines of previously established protocols[10, 11]. A roughly cylindrical brass rod (weight 313 g; applied diameter 1cm) was heated to 75 °C in a water bath. Three burns were then placed on the contralateral portions of the skin on the back for 5, 20, and 30 seconds. No additional pressure was applied to the rod while in contact with the skin other than that supplied by gravity.

The burns were then scanned with the PS-OCT device. Scans were cross-sectional and approximately 3 mm long by 2 mm deep. Tissue was taken from the scanned region using 4 mm punch biopsies (Miltex, Lake Success, NY), and then processed with a regressive hematoxylin and eosin (H&E) stain for histopathologic analysis. A PS-OCT scan and biopsy were taken of normal skin as a control. Animals were then euthanized.

2.2. PS-OCT system

The PS-OCT system used in the previous study was a free space interferometer composed of bulk optical components. This allows for precise control of the polarization state of the light in the reference arm and incident in the sample arm, but required considerable alignment before use. The fiber-based system eases the alignment procedure. It also makes reorientation of the sample arm possible; the rats were placed directly below a vertically oriented sample arm, whereas a horizontal orientation can be easier for scanning larger objects. However, the inherent birefringence in an optical fiber can alter the polarization state of light transmitted through it and must be compensated for. Polarization-maintaining fibers do exist, but phase information between wave components of light, critical to our analysis, is lost. The fibers used in the system (Corning SMF-28) are single mode and have polarization mode dispersion (PMD) caused by stress and imperfections in fiber core circularity. PMD of these fibers is less than 0.5 ps / $\sqrt{\text{km}}$ and phase information is preserved as these fibers maintain an optical path length difference between orthogonal polarization states of less than 10 μm for 4 meters of fiber.

A diagram of the high-speed fiber-based PS-OCT system is shown in Figure 1a. A low coherence source (AFC Technologies) with a FWHM bandwidth of 80 nm centered at 1.3 μm is sent through quarter and half wave plates to select the polarization state of the source with the highest power. This light is sent through a bulk polarizer and then another set of quarter and half wave plates before being coupled into single mode fiber. The wave plates are adjusted so that the light that emerges from the fiber has equal magnitude wave components parallel and perpendicular to the optic axis of an electro-optic polarization modulator (New Focus 4104). A four step driving function controls the modulator to alter the polarization state in $\pi/2$ increments spanning a grand circle on Poincaré's sphere (Figure 1b). A 2x2 fiber splitter sends the light to the reference and sample arms. The sample arm consists of a single mode fiber with a collimator and focusing lens mounted on a motorized translation stage. In the reference arm, the light is passed through a static polarization controller (General Photonics) and a PM fiber pigtailed phase modulator (JDS Uniphase) and sent into a rapid scanning optical delay line (RSOD)[12, 13]. The RSOD is operated with the spectrum centered on a galvo-mounted mirror to generate a group delay with no phase delay, changing the apparent path length of the reference arm. The RSOD is controlled with a triangular waveform at 624 Hz. The carrier frequency is generated by the phase modulator. The light from the two arms is sent back through the splitter and into the detection arm. This consists of a static polarization controller, a fiber pigtailed polarizing beam splitter, and two detectors. The signal is high pass filtered, amplified, and digitized before being used to calculate the Stokes parameters of the light[14].

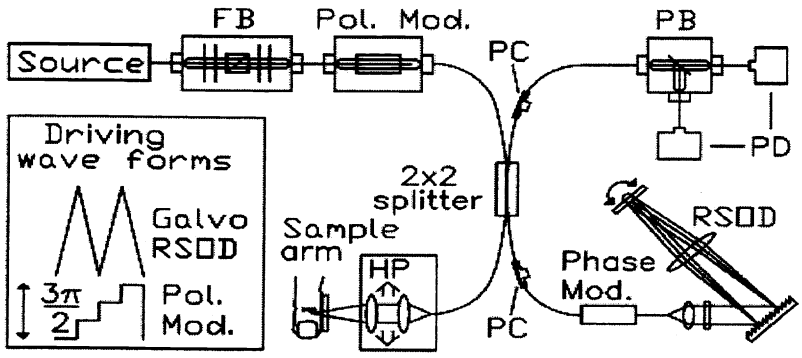

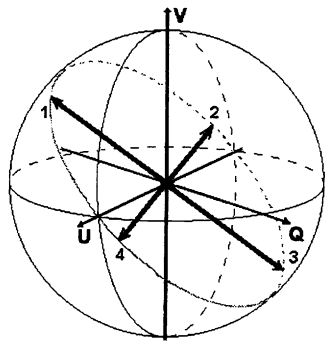

Figure 1a: Fiber-based PS-OCT setup. FB: fiber bench with polarizer, Pol. Mod.: polarization modulator, PC: static polarization controller, PB: polarizing beam splitter, RSOD: rapid scanning optical delay line, PD: photodiodes, HP: handpiece on motorized linear translation stage (velocity 1.87 mm/sec).

Figure 1b: The four orthogonal polarizations of light at the fiber tip used to probe the sample exist within a grand circle in Poincaré's sphere.

2.2.1. PS-OCT analysis procedure

The four orthogonal orientations of light used to probe the sample exist within a grand circle in Poincaré's sphere (Figure 1b). Since polarizations 1 and 3 differ only by a minus sign in the Q, U, and V Stokes parameters, they contain the same information, as do polarizations 2 and 4. The information is averaged to reduce noise and to obtain two sets of independent Stokes vectors.

The sample surface can be found by using the large intensity signal (the I Stokes parameter) reflected from the tissue surface. The polarization state of the light at the surface in any given A-line is taken as the incident polarization of the light on the sample. This is a necessary calculation because the stress and imperfections in fiber core circularity can introduce a constant, but unknown, degree of linear and circular birefringence. By comparing the surface reflection to the polarization state of light at a particular depth in the same A-line, the fiber birefringence can be eliminated and it is possible to calculate a plane in which the optic axis must reside. Intersection of planes resulting from two different polarization input states yields a single optic axis. The degree of phase retardation about that optic axis must now be calculated.

For any single input state, the degree of phase retardation can be calculated exactly. That is, the angle required to rotate the incident polarization about the optic axis to the polarization state at the point in question can be calculated analytically. In practice, the phase retardations calculated from the two input states will differ, necessitating an optimization procedure. A single measure of the degree of phase retardation is found by minimizing the intensity-weighted average of the deviation between rotated incident light and the true polarization state for the two input states simultaneously. These images are then averaged over A-lines to yield plots of phase retardation versus depth below the tissue surface. The slopes of the roughly linear portions of the plots were reported.

2.3. Histological Analysis

Histological analysis was used to determine the true burn depth. There were three main criteria used to make this determination. The first was examination of the state of viable adnexal structures, such as hair follicles and sweat glands[15]. If such structures appeared damaged, it can be inferred that thermal injury reached at least that depth. A second criterion was the color of the histological section. The regressive H&E stain goes from a pink color in normal skin to a purple in the presence of denatured dermal collagen. A final criteria was the presence of hyalinization[15, 16]. Normal dermis is composed of collagen fibers and fibroblasts oriented roughly parallel to the skin surface. When the skin is thermally damaged, the fibers lose their linearity, fusing with their neighbors to create a glass-like appearance from the dense coagulations of collagen. Signs of this hyalinization were taken to indicate that thermal injury had occurred to that depth. The slides were placed under an Olympus BH-2 microscope with a reticle eyepiece. Using the ruler built into the microscope, the actual burn depth in

micrometers (± 5μm) was measured according to the previously mentioned criteria for each histological section. The burn depth reported is the average of the individual measurements of all sections taken from a particular biopsy. Histological analysis was done independently of the PS-OCT scan analysis.

3. RESULTS

Figures 2 and 3 show normal and burned rat skin, respectively. Figure 2a and 3a are histological sections and comparison between the two highlights some of the criterion used in burn depth determination. The clearest difference in the general appearance of the tissue is the presence of hyalinization. The normal skin in Figure 2a has a fairly uniform density of collagen fibers throughout the dermal layer. These same collagen formations are not visible in the upper regions of Figure 3a, resulting in a coagulated appearance.

The phase maps (Figures 2b and 3b) are encoded such that the darker regions correspond to 0° difference compared to the incident light and white to 180°. In the burned tissue, the darker region extends to a visibly greater depth than in normal skin, indicating a lesser degree of birefringence in the corresponding tissue. This difference is quantified in the phase retardance plots (Figures 2c and 3c) averaged over all A-lines, with depths measured from the tissue surface. The burned skin shows a clearly lower slope in the linear portions of the plots. Figure 5 summarizes the experimental results. The phase retardation of each point is the average (n=3) of the slopes obtained for the 5, 20, and 30 second burns and the burn depth is the average burn depth as determined by histological analysis. Error bars are determined by the standard deviations of the individual measurements.

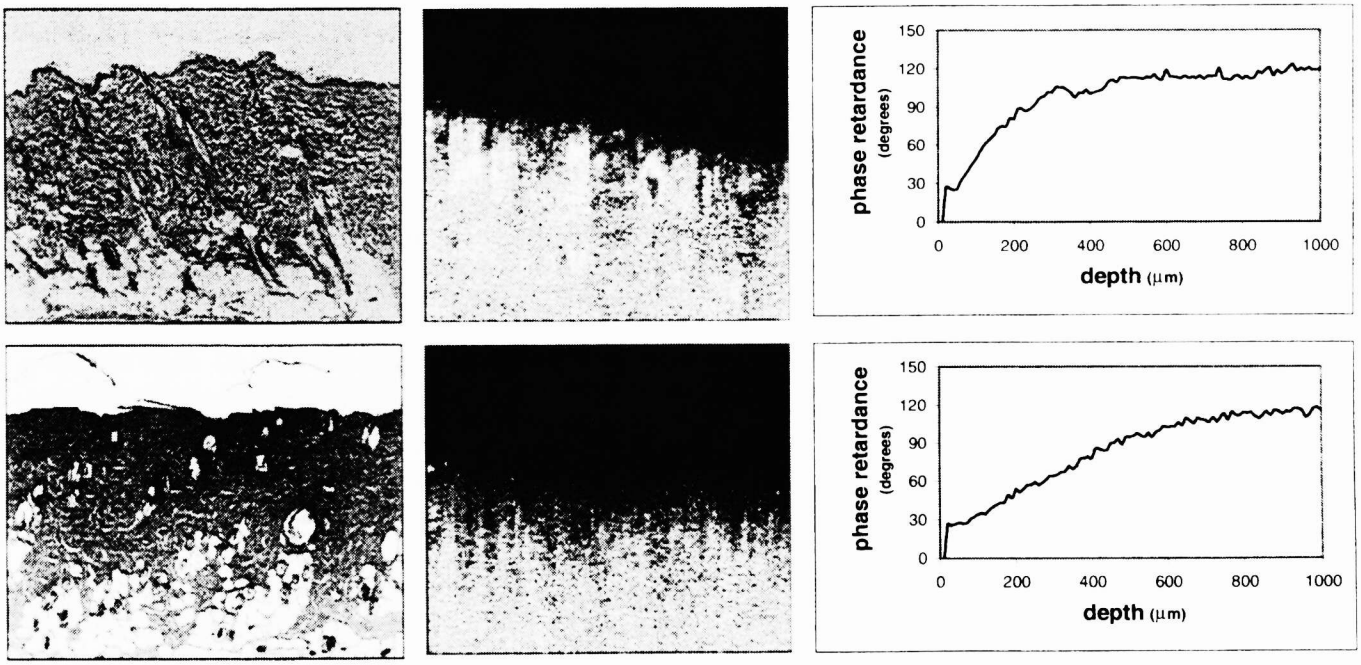

Figure 2: Normal rat skin. (a) histology (b) phase map (c) graph of phase retardance vs. depth.
Figure 3: Rat skin burned at 75°C for 30 seconds. (a) histology (b) phase map (c) graph of phase retardance vs. depth.
The dimensions of the histological images and phase maps are 3.2 mm by 2 mm, and depths in the graphs are measured from the surface of the tissue.

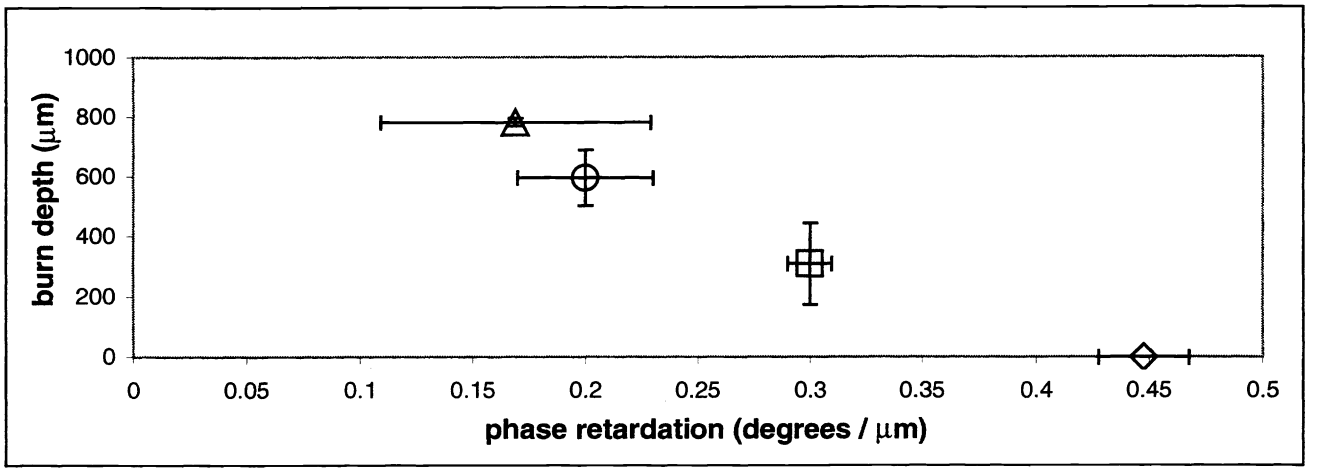

Figure 4: Overall graph of phase retardation from PS-OCT vs. burn depth from histology (n=3 for all points). The diamond represents normal rat skin. The square, circle, and triangle correspond to skin burned for 5, 20, and 30 seconds at 75°, respectively.

4. DISCUSSION

Birefringence in human skin comes from collagen. Collagen is a weakly birefringent material with a fairly uniform distribution in skin. Therefore, when light travels through more skin, it has traveled through more collagen and should show signs of more phase retardation. Examination of Figure 2c demonstrates this in normal rat skin. In the first 300 μm, as the depth increases, the average phase retardation also increases. At a depth of 500 μm, the phase retardation has leveled off to approximately 115°. One possible explanation for this behavior is depolarization due to scattering. As the depth of the scan increases, the effects of scattering become more pronounced. Scattering reduces the intensity and randomizes the polarization of the light. Monte Carlo simulation of this effect yields a phase retardation at the higher depths of 114.9° ± 0.1°.

The phase retardation plot for the burned skin can be explained by collagen denaturation[15]. It has been demonstrated that collagen denatures at temperatures between 56-65°C. At these higher temperatures, the molecules become isotropic, resulting in lower birefringence[8]. It should then be expected that burned skin would have a lower phase retardation per micrometer of depth. This is clearly demonstrated in Figure 3c, as the slope in the linear portion is much lower than that in the unburned skin.

Figure 4 shows a clear correlation between the information obtained from PS-OCT and the histologically determined burn depth. As burn depth increases, the phase retardation per unit depth decreases. The relative size of the error bars is also informative. Since the birefringence in the tissue is reduced in deeper burns, scattering will contribute more to the overall change in polarization. The depolarization due to scattering is random, resulting in an increasing variation in phase retardation per unit depth. It should also be noted that the error in the burn depth reported at 30-seconds is remarkably smaller than that for the 20- or 5-second burns. This can be attributed to the fact that the histological analysis can only measure damage in the dermal layer, observed here to be slightly greater than 800 μm in depth. This limits the reportable burn depth, whereas the burn probably extends into the subcutaneous fat.

The preliminary experiments (n=3) show a clear correlation between burn depth and phase retardation. A potential problem is limited penetration depth in the scans, but information can be extrapolated beyond the measurement area. The first millimeter of skin in which the burn depth has reached two millimeters should show lower birefringence than that in which the full extent of the burn is one millimeter. Being able to image faster to a greater depth is the preferable option, and so as PS-OCT evolves, it will become more useful in the clinical diagnosis of thermal injury.

ACKNOWLEDGEMENTS

The authors would like to thank Leacky Liaw for her expertise in histology and Laurie Newman for her assistance with animal handling. This study was done with the support of the Whitaker Foundation (WF-26083), ONR, DOE, and NIH.

REFERENCES

1. P.A. Brigham and E. McLoughlin, "Burn incidence and medical care use in the United States: estimates, trends, and data sources," *J. Burn Care Rehabil.* **17**: pp. 95-107, 1997.
2. R.L Sheridan, KT Schomaker, L.C. Lucchina, et al., "Burn depth estimation by use of indocyanine green fluorescence: initial human trial," *J. Burn Care Rehabil.* **16**: pp. 602-4, 1995.
3. D. Heimbach, L. Engrav, B. Grube, and J. Marvin, "Burn depth: a review," *World J. Surg.* **16**: pp. 10-15, 1992.
4. D.H. Park, J.W. Hwang, K.S. Jang, D.G. Han, K.Y. Ahn, and B.S. Baik, "Use of laser Doppler flowmetry for estimation of the depth of burns," *Plast. Reconstr. Surg.* **101**: pp. 1516-23, 1998.
5. E.K. Yeong, R. Mann, M. Goldberg, L. Engrav, and D. Heimbach, "Improved accuracy of burn wound assessment using laser Doppler," *J. Trauma* **40**: pp. 956-62, 1996.
6. J.F. de Boer, T.E. Milner, M.J.C. van Gemert, and J.S. Nelson, "Two-dimensional birefringence imaging in biological tissue by polarization-sensitive optical coherence tomography," *Opt. Lett.* **22**: 934-6, 1997.
7. M.J. Everett, K. Schoenenberger, B.W. Colston, and L.B. da Silva, "Birefringence characterization of biological tissue by use of optical coherence tomography," *Opt. Lett.* **23**: pp. 228-30, 1998.
8. J.F. de Boer, S.M. Srinivas, A. Malekafzali, Z. Chen, and J.S. Nelson, "Imaging thermally damaged tissue by polarization sensitive optical coherence tomography," *Optics Express* **3**, pp. 212-8, 1998.
9. S.M. Srinivas, J.F. de Boer, B.H. Park, K. Keikhanzadeh, H.L. Huang, Z. Chen, and J.S. Nelson, "Determination of burn depth by polarization sensitive optical coherence tomography," *(submitted)*.
10. J. Smahel, "Viability of skin subjected to deep partial skin thickness thermal damage: experimental studies," *Burns* **17**, pp. 17-24, 1991.
11. T. Kaufman, S.N. Lusthaus, U. Sagher, and M.R. Wexler, "Deep partial skin thickness burns: a reproducible animal model to study burn wound healing," *Burns* **16**, pp. 13-16, 1990.
12. G.J. Tearney, B.E. Bouma, and J.G. Fujimoto, "High speed phase and group delay scanning with a grating based phase control delay line," *Opt. Lett.* **22**: pp. 1811-3, 1997.
13. A.M. Rollins, M.D. Kulkarni, and S. Yazdanfar, "*In vivo* video rate optical coherence tomography," *Opt. Lett.* **3**: pp. 219-29, 1998.
14. J.F. de Boer, T.E. Milner, J.S. Nelson, "Determination of the depth-resolved Stokes parameters of light backscattered from turbid media by use of polarization-sensitive optical coherence tomography," *Opt. Lett.* **24**: pp. 300-2, 1999.
15. T.W. Panke, C.G. McLeod, *Pathology of thermal injury: a practical approach*, Grune & Stratton, Inc., Orlando, FL, 1985.
16. S. Thomsen, "Pathologic analysis of photothermal and photomechanical effects of laser-tissue interactions," *Photochem. Photobiol.* **53**, pp. 825-35, 1991.